ADVANCED FUNCTIONAL MATERIALS
www.afm-journal.de

Luminescent Metal-Organic Frameworks for Selectively Sensing Nitric Oxide in an Aqueous Solution and in Living Cells

Pengyan Wu, Jian Wang, Cheng He, Xiaolin Zhang, Yanting Wang, Tao Liu, and Chunying Duan**

Cu^{2+}-based metal-organic framework (Cu–TCA) (H_3TCA = tricarboxytriphenyl amine) having triphenylamine emitters was assembled and structurally characterized. Cu–TCA features a three-dimensional porous structure consolidated by the well-established $Cu_2(O_2CR)_4$ paddlewheel units with volume of the cavities approximately 4000 nm^3. Having paramagnetic Cu^{2+} ions to quench the luminescence of triphenylamine, Cu–TCA only exhibited very weak emission at 430 nm; upon the addition of NO up to 0.1 mM, the luminescence was recovered directly and provided about 700-fold fluorescent enhancement. The luminescence detection exhibited high selectivity – other reactive species present in biological systems, including H_2O_2, NO_3^-, NO_2^-, $ONOO^-$, ClO^- and $^1O_2$, did not interfere with the NO detection. The brightness of the emission of Cu–TCA also led to its successful application in the biological imaging of NO in living cells. As a comparison, lanthanide metal-organic framework Eu–TCA having triphenylamine emitters and characteristic europium emitters was also assembled. Eu–TCA exhibited ratiometric fluorescent responses towards NO with the europium luminescence maintained as the internal standard and the triphenylamine emission exhibited more than 1000-fold enhancement.

1. Introduction

Molecular recognition is one of the most important processes in biological and chemical systems and governs the diverse functions and unique properties of a variety enzymes and synthetic receptors.[1] Since molecular recognition is operated through non-covalent interaction algorithms between receptors and substrates, the design and assembly of synthetic receptors mimicking biological systems to discriminate different substrates with high efficiency and selectivity is a critical and challenging task.[2] Porous metal–organic frameworks (PMOFs) represents a new class of inorganic–organic supramolecular hybrid materials comprising ordered networks formed from organic electron donor linkers and metal cations.[3] Their tunable pore size and characteristic functionality that are similar to active sites in proteins suggests they may act as bright promising host matrices for molecular recognition,[4] because the inherent confinement effect within their pores serves as preconcentrator to enhance the host-guest interactions and the pore surface designability enables the incorporation of appropriate specific interaction sites into a scaffold through the use of strategic organic chemistry.[5] Recent investigations also suggest that the specific, unique molecular recognition between porous MOFs and guest substrates is the design criteria to construct porous MOFs with functional pores to direct the functions and applications.[6] In this case, the combination of signal transduction pathways and accessible porosity within these MOFs materials will impart them with the capability of transducing the host–guest behavior to detectable changes, porous MOFs thus are postulated as excellent candidates for chemical sensing applications.[7] And the general strategy for increasing selectivity and sensitivity of porous MOFs not only includes enhancing the level of sophistication in the recognition unit for a target molecule by optimizing the host-guest interactions, but also involves improving the signal transduction mechanism that directly visualizes the host-guest interaction.[8]

On the other hand, nitric oxide (NO) is an important mediator of both physiological and patho-physiological processes and a key player in numerous mammalian functions, including vasodilation, immune responses, and neurotransmission, and has also been recognized as an atmospheric pollutant and a potential health hazard.[9] Due to its large diffusivity and high reactivity with other radicals and metal-containing proteins in biological systems, the development of methods capable of detecting NO in biology has been an intriguing challenge for chemists, biologists and engineers.[10] It has also been postulated that various biological and physiological reactivities of nitric oxide are attributed to the formation of nitrosyl complexes of metalloproteins, mostly iron or copper protein;[11]

Dr. P. Wu, J. Wang, C. He, X. Zhang, Y. Wang, T. Liu, Prof. C. Duan
State Key Laboratory of Fine Chemicals
Dalian University of Technology
Dalian, 116012, China
E-mail: liutao@dlut.edu.cn; cyduan@dlut.edu.cn

DOI: 10.1002/adfm.201102157

the chemistry of NO coordination thus provides a mechanism by which metal complexes react with NO and has also been employed as a powerful strategy for NO sensing.[12] These transition metal based sensors permit the identification of NO from both inducible and constitutive forms of nitric oxide synthase and facilitate the investigation of different NO functions in response to external stimuli.[13] Recently, a number of metal–organic frameworks materials have been proposed as delivery agents for exogenous NO.[14] The whole adsorption–storage–delivery cycle indicates that MOFs reported can deliver pure gaseous NO in high quantities, confirming their applicability as potential gas storage materials for energy, environmental, and biological applications. Herein, through incorporating triphenylamine moiety as an efficient emitter,[15] we report Cu^{2+}-based metal-organic framework Cu–TCA (H_3TCA = tricarboxytriphenyl amine), to realize the applications of MOFs in the luminescent detection of NO. We reasoned that the paramagnetic characteristics of Cu^{2+} ions would quench the ligand-based fluorescence completely, while the coordination of NO to the metal ions exposed on the surface of the MOF would thus reduce Cu^{2+} centers to Cu^{+} to recover the luminescence directly.[16]

2. Results and Discussion

2.1. Synthesis and Characterization of Cu–TCA

Solvothermal reaction of H_3TCA and $Cu(NO_3)_2 \cdot 6H_2O$ in mixed solvents of DMF and methanol gave compound Cu–TCA in a high yield (70%). Elemental analyses (EA) along with the powder X-ray analysis indicated the pure phase of its bulky sample (Figure S1, Supporting Information). Single crystal structure analysis revealed that topology of Cu–TCA framework was similar to that of the porous metal–organic framework HKUST-1.[17] It was composed of paddle wheel dinuclear Cu_2 units with a short Cu–Cu internuclear separation of 2.063(4) Å, bridged by four TCA^{3-}. Moreover, each TCA^{3-} ligand connected three dinuclear Cu_2 units to form a non-interpenetrating 3D network. Each copper ion in the paddlewheel SBU was coordinated with four symmetric-related oxygen atoms from four respective carboxylates and one axial water molecule opposite to the Cu–Cu vector. The overall framework of Cu–TCA consists of large truncated cubic "cages" delimited by 8 TCA^{3-} ligands and 12 $Cu_2(O_2CR)_4$ paddlewheel SBUs. Using the central N atoms as the points of the cage, its radii is about 1.0 nm. (**Figure 1**)

The free volume in fully desolvated Cu–TCA was estimated to be approximately 79.7% by PLATON software, and TGA analyses also showed that the Cu–TCA exhibited an impressive solvent weight loss of 52.5 weight percent (wt%) in the temperature range 25–200 °C (Figure S2, Supporting Information), which confirmed the highly open framework structure. Simultaneously, dye-uptake studies by soaking the Cu–TCA in a solution of Brilliant Blue R-250 (BBR-250) dye in methanol for 24 hours,[18] the dye uptake, which was approximately 34% of the framework weight, was examined (Figure S3, Supporting Information). Experimental results demonstrated conclusively the accessibility of the small molecular to the MOF through the open channels.

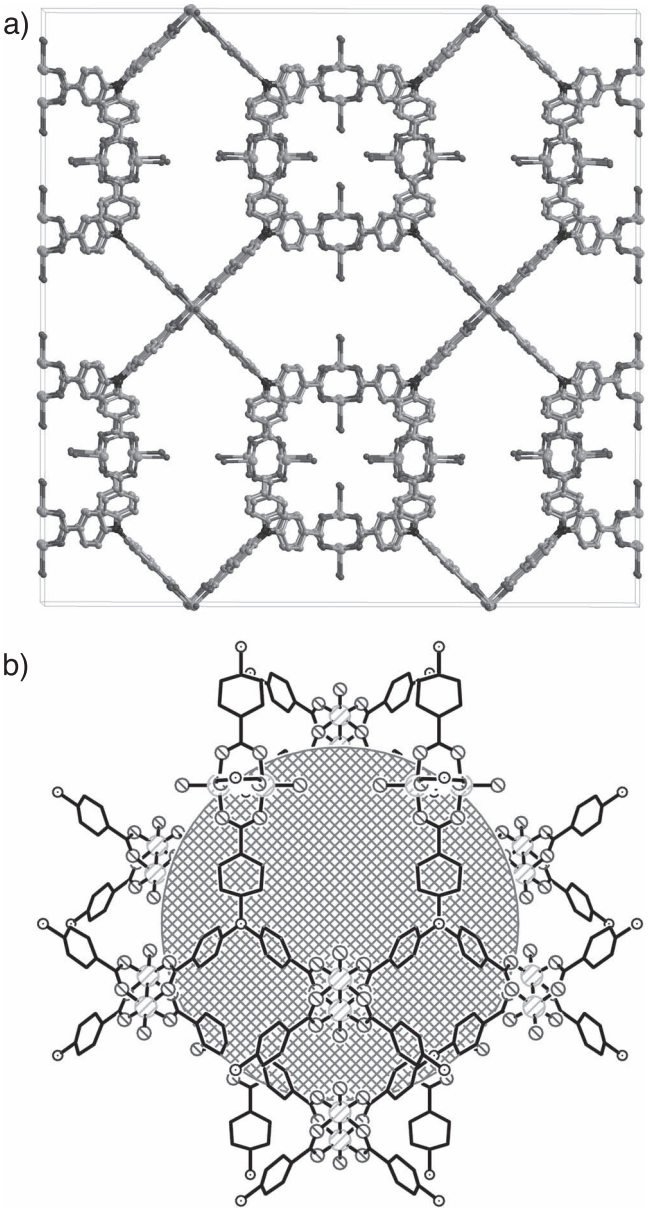

Figure 1. View of the crystal packing of Cu–TCA along *a* direction showing the rhombus channels with the coordinated unsaturated metal ions and nitrogen atoms exposed within the channels and coordination configuration of the metal center, and the truncated cubic consisted unit in Cu–TCA.

2.2. Fluorescence and Mechanism Studies of Cu–TCA with NO

Cu–TCA exhibited absorption bands centered at 350 nm assignable to the π–π^* transition of the triphenylamine group.[19] The ligand exhibited photoluminescence at about 430 nm when excited at 350 nm, whereas the emission of the ligand reduced in the Cu(II)-based MOF due to the quenching of paramagnetic center. As can be expected, the introduction of excess NO to the suspension of Cu–TCA caused a significant increase in fluorescence, since reduction of Cu(II) to form a diamagnetic species Cu(I) can alleviate quenching caused by paramagnetic metal ions during

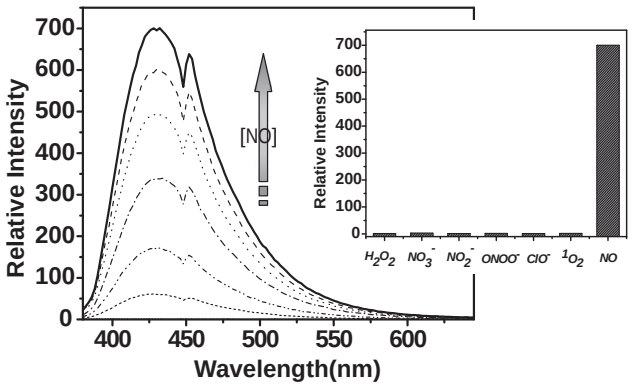

Figure 2. Family of Cu–TCA emission spectra treated with NO concentration: 0.0 mM (short dot line), 0.3 mM (short dash line), 0.5 mM (dash dot dot line), 0.6 mM (dash dot line), 0.7 mM (dot line), 0.8 mM (dash line), 1 mM (solid line) at room temperature in CH_3CN/Tris buffer (7/3, v/v, pH = 7.4, Tris = trishydroxy methyl aminomethan). The insert shows the luminescence intensities of the products of Cu–TCA treated with various ROS and RNS in CH_3CN/Tris buffer. NO: 1 mM; H_2O_2: 5 mM; NO_3^-: 5 mM $NaNO_3$; NO_2^-: 5 mM $NaNO_2$; $ONOO^-$: 5 mM NaONOO; OCl^-: 5 mM NaOCl; $^1O_2$: 5 mM H_2O_2 + 5 mM NaOCl.

this process. Consequently, A 700-fold increase in fluorescence was observed when Cu–TCA was allowed to react with 1 mM NO (**Figure 2**), indicating the potential of Cu–TCA for NO sensing. In a control experiment, a free ligand solution treated with excess NO only showed a small increase (10%) in fluorescence.

To evaluate the reaction specificity of Cu–TCA with NO under physiological conditions, a wide array of possible competitive reactive oxygen and nitrogen species and other analytes up to five-fold excess were screened. As depicted in Figure 2, no detectable responses appeared upon the addition of 5 equiv. of ClO^-, NO_2^-, NO_3^-, H_2O_2, $ONOO^-$ and $^1O_2$, whereas the luminescence intensity was increased significantly after treatment with NO solution. This result demonstrated that the fluorescence response of Cu–TCA was specific for NO.

The electron paramagnetic resonance (EPR), Fourier transform infrared (FT–IR) spectroscopy and fluorescence lifetime experiment were carried out to investigate the mechanism of the emission turn-on of Cu–TCA by NO. The EPR spectra of Cu–TCA exhibited the characteristic signal of Cu(II) at 3000 and 3296 Gauss. Subsequently, the addition of NO led to the suppression of EPR features for Cu–TCA in the solution confirming the formation of a Cu(I) species (Figure S4, Supporting Information).[20] The formation of a diamagnetic Cu(I) complex during the reaction between NO and Cu(II) complexes can recover the quenched fluorescence of a triphenylamine coordinated to the paramagnetic metal. Moreover, putting Cu–TCA into the DMF saturated solution of NO for 3 hours afforded new crystalline solids. The IR spectrum displayed two new bands at 1683 cm^{-1} and 1763 cm^{-1} indicating the presence of the antisymmetric and symmetric N-O stretching of Cu(I)–NO adducts (Figure S5, Supporting Information).[21] Time-resolved emission measurements were used to further probe the interaction between Cu–TCA and NO, and emission decay curves are shown in Figure S6, Supporting Information. Emission decays for Cu–TCA were best fit by a monoexponential function with 0.23 ns, attributed to emission from tricarboxytriphenyl amine in the presence of Cu^{2+}. Putting Cu–TCA into the DMF saturated solution of NO for 3 hours afforded new crystalline solids of which emission decays were fit best by a biexponential function. The faster component has ι = 0.47 ns, was similar to the original one, likely due to Cu^{2+} quenched emission from tricarboxytriphenyl amine units. And the presence of a new relative longer-lived species, with a lifetime of 2.61 ns, suggested part of the Cu(II) centers were reduced to Cu(I) in the presence of NO, resulting in the quenching of the ligand excited state being blocked.[22] The experimental results demonstrated that Cu–TCA was capable of fluorescent NO detection via NO-induced metal reduction accompanied by concomitant fluorescence enhancement.

2.3. Luminescence Imaging of Cu–TCA

The high selectivity coupled with the solubility in aqueous media of Cu–TCA made it a superior probe for NO detection via biological imaging. Remarkably, MOFs need to be scaled down to the nanoregime to form nanoscale metal-organic frameworks (NMOFs) to be used as delivery vehicles for imaging agents and drug molecules.[23] The dark green, crystalline nanoparticles of Cu–TCA (NCu–TCA) were synthesized in 30% yield by microwave heating of a solution of H_3TCA and $Cu(NO_3)_2$ in DMF/CH_3OH at 100° for 5 min. The SEM images showed that NCu–TCA forms block-like particles with dimensions of approximately 100 nm × 100 nm × 100 nm (Figure S7, Supporting Information). PXRD studies indicate that the Cu–TCA particles are crystalline and share the same phase as the bulk crystals of Cu–TCA. (Figure S1, Supporting Information) MCF-7 cells were incubated for 30 min with 5 ppm NCu–TCA at 37° to allow the probe to permeate into the cells. The cells gave no intracellular fluorescence under selective excitation with blue light (350–400 nm) (**Figure 3**a). Subsequently, a significant blue fluorescence in the live cells was observed after the cells stained with suspension containing NCu–TCA were washed three times with Tris buffer, and then incubated with sodium nitroprusside (2.0 mM) for another 20 minutes (Figure 3c). Bright-field measurement confirmed that the cells after treatment with the probes solution and NO were viable throughout the imaging experiments (Figure 3d). These experiments indicate that our system could be used to monitor intracellular nitric oxide. In addition, we believe our results with Cu–TCA were the first example of metal-organic frameworks implicated biological imaging of NO in the living cells.

2.4. Ratiometric Luminescence Responses Towards NO by Eu–TCA: Synthesis, Characterization and Sensing Studies

The interesting imaging behavior of Cu–TCA encouraged us to further investigate the recognition behavior of the MOFs assembled by the triphenylamine moiety, compound Eu–TCA was produced by the hydrothermal reaction by using europium nitrate and H_3TCA. X-ray crystallography reveals that Eu–TCA crystallizes in the space group P2(1)/c. The asymmetry unit of

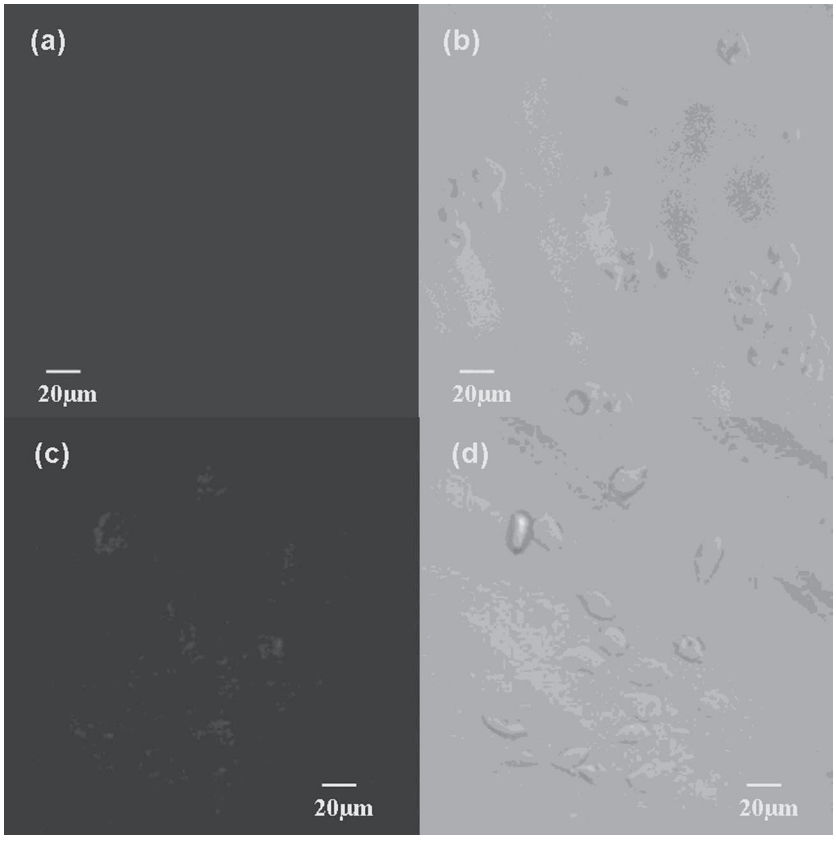

Figure 3. Fluorescence imaging response of Cu–TCA (5 ppm, suspended in Tris buffer) induced by sodium nitroprusside (2.0 mM). a) Fluorescence image of MCF-7 cells incubated with Cu–TCA. b) Brightfield image of cells shown in panel (a). c) Cells incubated with sodium nitroprusside. d) Brightfield image of cells shown in panel (c). Excited with blue light.

Eu–TCA contains three europium centers, three TCA^{3-} ligands and three coordinated H_2O molecules. Two of the Eu atoms adopt distorted dodecagonal coordination geometries with eight oxygen atoms from six carboxylate groups of TCA^{3-} or seven oxygen atoms from six carboxylate groups of TCA^{3-} and one H_2O. The third Eu center is coordinated by seven oxygen atoms from six carboxylate groups of TCA^{3-} and two terminal H_2O ligands. Each TCA^{3-} ligand coordinates to five different Eu^{3+} ions through two different coordination modes: bidentate and chelating/bisbridging bidentate. The eight- and nine-coordinate Eu^{3+} ions are linked together by carboxylate groups of TCA^{3-} to construct 1D Eu–O–C chains running along the [001] direction. These Eu–O–C chains, as rod-shaped SBUs, are interconnected through triphenylamine groups of TCA^{3-} to generate a 3D noninterpenetrating extended network with 1D rhombus channels of 7.5 × 8.5 $Å^2$ (measured between opposite atoms) viewed along the [001] direction (**Figure 4**). The metal centers have removable solvent molecules that are also well-positioned in the channels to interact with guest molecules that enter the framework pores to recognize small molecules.[24]

Given that triphenylamine emitter is an efficient sensitizer to prompt the corresponding luminescence, Eu–TCA exhibits characteristic Eu^{3+} emissions assignable to the transitions of $^5D_0 \rightarrow {}^7F_1$, $^5D_0 \rightarrow {}^7F_2$ and $^5D_0 \rightarrow {}^7F_4$ when excited at 350 nm,[25] beside the emission of the triphenylamine group centered at about 430 nm. A fluorescence titration with the DMF saturated solution of NO was conducted on a suspension of Eu–TCA (4 ppm) in acetonitrile. Upon addition of NO solution, the luminescence intensity of Eu–TCA at 430 nm increased gradually with the enhanced efficiency up to 1620-fold. Interestingly, the intensity of emission at 610 nm remained virtually unchanged.

Thus, Eu^{3+} emission could act as internal standard to determine the concentration fraction of the host-guest species since no significant spectral changes were found corresponding to the characteristic Eu^{3+} emission.[26] The ratio of the emission intensities at 430 nm and 610 nm (I_{430}/I_{610}) became constant when the amount of the added NO reached 140 μM (**Figure 5**a). Moreover, the emerged ratiometric chemosensor is quite significant since it can eliminate most or all ambiguities by self-calibration between two emission bands.[27] Accordingly, the spectral responses upon addition of NO could be assigned to the formation of coordination bonds between the europium and NO, due to the new peak of the mononitrosyl (Eu–NO) at 1927 cm^{-1} observed in the FT–IR spectrum (Figure S8).[28]

The fluorescence response of the Eu–TCA probe is also specific for NO over other reactive species present in biological systems, including H_2O_2, NO_3^-, NO_2^-, $ONOO^-$, ClO^- and $^1O_2$. However, since Eu–TCA is very sensitive to water,[29] that is, fluorescence quenching in the presence of water, its application on fluorescence imaging in biological system is further limited.

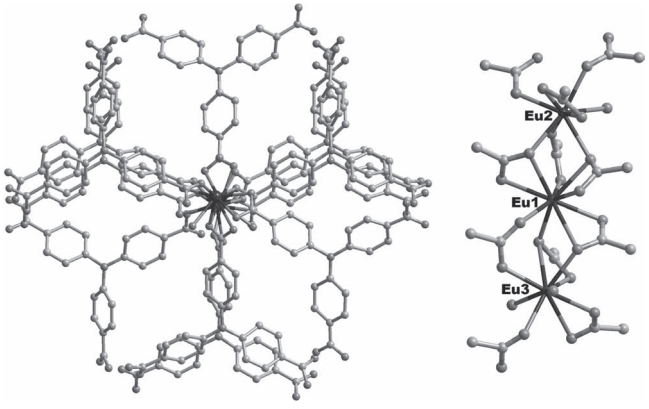

Figure 4. View of Eu–TCA crystal packing along *c* direction showing the rhombus channels with the coordinated unsaturated metal ions and nitrogen atoms exposed within the channels and coordination configuration of the metal center. The metal, oxygen, nitrogen and carbon atoms are drawn in shades of grey.

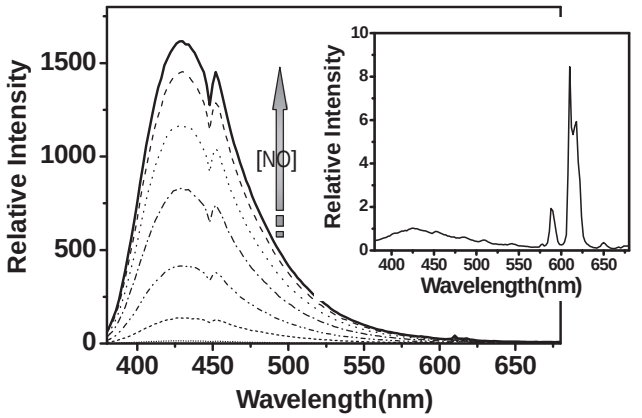

Figure 5. The family of Eu–TCA emission spectra with NO concentration: 0.00 mM (short dot line), 0.03 mM (short dash line), 0.05 mM (dash dot dot line), 0.07 mM (dash dot line), 0.09 mM (dot line), 0.11 mM (dash line), 0.13 mM (solid line) at room temperature in CH_3CN. Insert: Emission spectra of Eu–TCA without NO. Excitation at 350 nm.

3. Conclusions

In summary, two new MOF-based NO chemosensors Cu–TCA and Eu–TCA are developed through incorporating triphenylamine moiety as a bright blue emitter. The coordination of NO to the Cu(II) ions of the MOF reduces Cu^{2+} centers to Cu^{+} and recover the luminescence in aqueous solution directly. Excellent selectivity and high sensitivity enables Cu–TCA to realize the applications of the bioimaging in living cells. Eu–TCA exhibited lanthanide-based emission (610 nm) and triphenylamine emission (430 nm) and worked as a ratiomeric luminescent chemosensor towards NO. We are now exploring some more selective and sensitive ratiometic luminescent MOFs, and developing the strategies to construct such microporous luminescent MOF nanoparticles, disperse them into a biological system and make use of optical fluorescent imaging technology for the sensing of NO.

4. Experimental Section

Material and Methods: Unless otherwise stated, all chemical materials were purchased from commercial sources and used without further purification. 4,4′,4″-tricarboxytriphenylamine was synthesized according to the published procedure.[S1] The saturated dimethylformamide solution of NO was prepared by passing NO gas through a argon-deoxidized DMF for 3 h. The NO concentration was measured by using the Griess method.[S2] ^{1}H NMR spectra were measured on a Varian INOVA 400M spectrometer. The powder XRD diffractograms were obtained on a Riguku D/Max-2400 X-ray Diffractometer with Cu sealed tube (λ = 1.54178 Å). Elemental analyses were obtained on Elemental Analyzer Vario EL iii. Thermogravimetric analysis (TGA) was carried out at a ramp rate of 5°/min in a nitrogen flow with a Mettler-Toledo TGA/SDTA851 instrument. FT-IR spectra were recorded as KBr pellets on JASCO FT/IR-430.

X-band EPR spectra were recorded on a Bruker EMX EPR spectrometer (9.45 GHz). Temperature control was performed with an Oxford Instruments ESR900 liquid-helium cryostat and ITC503 controller. Cu–TCA (10 mg) set in the DMF saturated solution of NO for 3 hours, was directly placed in an EPR tube for EPR determination at the room temperature.

Fluorescence spectra of the solution were obtained using the FLS920 spectrometer (Edinburgh Instruments). Both excitation and emission slit were 3 nm wide. Fluorescence measurements were carried out in a 1 cm quartz cuvette on a suspension of Cu–TCA in acetonitrile/Tris buffer (pH = 7.4) excited at 350 nm with cuvette solutions protected by argon atmosphere. The luminescence of Eu–TCA was examined in acetonitrile under argon atmosphere, and the intensity was recorded at 430 nm and 610 nm, excited at 350 nm.

Cells images were captured using the Nikon eclipase TE2000-5 inverted fluorescence microscopy. MCF-7 cells were cultured in 1640 supplemented with 10% FCS. MCF-7 cells were seeded in 24-well flat-bottomed plates. Then they were maintained at 37° in a 5% CO_2/95% air incubator for 12 h.

Synthesis and Crystal Growth: Cu–TCA: A mixture of 4,4′,4″-tricarboxytriphenylamine (H_3TCA) (94 mg, 0.25 mmol) and $Cu(NO_3)_2{\cdot}6H_2O$ (242 mg, 1 mmol) were dissolved in 15 mL mixed solvents of DMF and methanol in a screw-capped vial. The resulting mixture was kept in an oven at 120 °C for 3 days. Green block-shaped crystals were obtained after filtration. Yield: 70%. Anal. calcd. for $Cu_3(C_{21}H_{12}NO_6)_2(H_2O)_3$ (dried vacuum%): C, 50.78; H, 3.04; N, 2.82; Found: C, 49.77; H 3.45, N 2.08. FTIR (KBr pellet): ν = 3427 (w), 1656 (m), 1596 (m), 1531 (m), 1507 (m), 1316 (m), 1276 (m), 1176 (m), 1102 (s), 1014 (s) cm^{-1}.

Eu–TCA: A mixture of 4,4′,4″-tricarboxytriphenylamine (H_3TCA) (94 mg, 0.25 mmol) and $Eu(NO_3)_3{\cdot}6H_2O$ (446 mg, 1 mmol) were dissolved in 15 mL mixed solvents of dimethyl formamide (DMF) and ethanol in a screw-capped vial. The resulting mixture was kept in an oven at 100° for 3 days. Yellow block-shaped crystals were obtained after filtration. Yield: 75%. Anal. calcd. for $Eu_3(C_{21}H_{12}NO_6)_3(H_2O)_3$ (dried vacuum%): C, 46.34; H, 2.59; N, 2.57; Found: C, 45.48; H 3.36, N 3.23. FTIR (KBr pellet): ν = 3431 (w), 1657 (m), 1592 (m), 1529 (m), 1507 (m), 1315 (m), 1175 (m), 1143 (s), 1102 (s), 1014 (s) cm^{-1}.

Crystallography: Crytallography intensities were collected on a Bruker SMART APEX CCD diffractometer with graphite monochromated Mo-Kα (λ = 0.71073 Å) using the SMART and SAINT programs. The structure was solved by direct methods and refined on F^2 by full-matrix least-squares methods with SHELXTL version 5.1.

Crystal data of Cu–TCA: $C_{55}H_{90}Cu_3N_2O_{32}$ [$Cu_3(C_{21}H_{12}NO_6)_2(H_2O)_3{\cdot}13CH_3OH{\cdot}4H_2O$], M = 1481.91, Cubic, space group Pm-3n, a = 23.211(3) Å, V = 12505(3) Å^3, Z = 4, Dc = 0.774 g cm^{-3}, μ(Mo-Kα) = 0.553 mm^{-1}, T = 180(2) K. 1980 unique reflections [R_{int} = 0.1286]. Final R_1 [with $I > 2\sigma(I)$] = 0.0792, wR_2 (all data) = 0.2031, GOOF = 1.020. CCDC number: 841879.

Crystal data of Eu–TCA: $C_{70.50}H_{64.5}Eu_3N_{5.50}O_{26}$ [$Eu_3(C_{21}H_{12}NO_6)_3(H_2O)_3{\cdot}2.5C_3H_7NO{\cdot}2.5H_2O$], M = 1860.66, Monoclinic, space group $P2_1/c$, a = 14.576(1) Å, b = 23.245(2) Å, c = 24.815(2) Å, β = 102.90 (1)°, V = 8195 (1) Å^3, Z = 4, Dc = 1.515 g cm^{-3}, μ(Mo-Kα) = 2.344 mm^{-1}, T = 298(2) K. 14359 unique reflections [R_{int} = 0.1127]. Final R_1 [with $I > 2\sigma(I)$] = 0.0738, wR_2 (all data) = 0.2153, GOOF = 0.962. CCDC number: 841880.

For both two data, non-hydrogen atoms of the ligand backbones were refined anisotropically. Hydrogen atoms within the ligand backbones were fixed geometrically at calculated positions and were allowed to ride on the parent non-hydrogen atoms.

Supporting Information

Supporting Information is available from the Wiley Online Library or from the author.

Acknowledgements

We gratefully acknowledge financial support from NSFC (Number: 21025102).

Received: September 12, 2011
Revised: December 13, 2011
Published online: February 6, 2012

[1] a) J. Rebek Jr., *Science* **1987**, *235*, 1478; b) R. M. Leblanc, *Curr. Opin. Chem. Biol.* **2006**, *10*, 529.
[2] a) B. Chen, S. Xiang, G. Qian, *Acc. Chem. Res.* **2010**, *43*, 1115; b) H. Chen, S. Ogo, R. H. Fish, *J. Am. Chem. Soc.* **1996**, *118*, 4993;

c) S. Ogo, S. Nakamura, H. Chen, K. Isobe, Y. Watanabe, R. H. Fish, *J. Org. Chem.* **1998**, *63*, 7151; d) R. Bakhtiar, H. Chen, S. Ogo, R. H. Fish, *Chem. Commun.* **1997**, 2135.

[3] a) O. M. Yaghi, M. O'Keeffe, N. W. Ockwig, H. K. Chae, M. Eddaoudi, J. Kim, *Nature* **2003**, *423*, 705; b) G. Ferey, *Chem. Soc. Rev.* **2008**, *37*, 191.

[4] a) B. Chen, Y. Yang, F. Zapata, G. Lin, G. Qian, E. B. Lobkovsky, *Adv. Mater.* **2007**, *19*, 1693; b) H.-L. Jiang, Y. Tatsu, Z.-H. Lu, Q. Xu, *J. Am. Chem. Soc.* **2010**, *132*, 5586.

[5] a) S. Horike, S. Shimomura, S. Kitagawa, *Nat. Chem.* **2009**, *1*, 695; b) R. Kitaura, S. Kitagawa, Y. Kubota, T. C. Kobayashi, K. Kindo, Y. Mita, A. Matsuo, M. Kobayashi, H.-C. Chang, T. C. Ozawa, M. Suzuki, M. Sakata, M. Takata, *Science* **2002**, *298*, 2358; c) J. S. Seo, D. Whang, H. Lee, S. I. Jun, J. Oh, Y. J. Jeon, K. Kim, *Nature* **2000**, *404*, 982; d) Z. Wang, S. M. Cohen, *Chem. Soc. Rev.* **2009**, *38*, 1315; e) W. J. Rieter, K. M. L. Taylor, W. Lin, *J. Am. Chem. Soc.* **2007**, *129*, 9852.

[6] B. Chen, L. Wang, Y. Xiao, F. R. Fronczek, M. Xue, Y. Cui, G. Qian, *Angew. Chem. Int. Ed.* **2009**, *48*, 500.

[7] a) A. Lan, K. Li, H. Wu, D. H. Olson, T. J. Emge, W. Ki, M. Hong, J. Li, *Angew. Chem. Int. Ed.* **2009**, *48*, 2334; b) B. Harbuzaru, A. Corma, F. Rey, P. Atienzar, J. Jorda, H. Garcia, D. Ananias, L. Carlos, R. Rocha, *Angew. Chem. Int. Ed.* **2008**, *47*, 1080.

[8] Y. Takashima, V. M. Martinez, S. Furukawa, M. Kondo, S. Shimomura, H. Uehara, M. Nakahama, K. Sugimoto, S. Kitagawa, *Nat. Commun.* **2011**, *2*, 168.

[9] T. Nagano, T. Yoshimura, *Chem. Rev.* **2002**, *102*, 1235.

[10] a) J. H. Kim, D. A. Heller, H. Jin, P. W. Barone, C. Song, J. Zhang, L. J. Trudel, G. N. Wogan, S. R. Tannenbaum, M. S. Strano, *Nat. Chem.* **2009**, *1*, 473; b) Y. J. Yang, S. K. Seidlits, M. M. Adams, V. M. Lynch, C. E. Schmidt, E. V. Anslyn, J. B. Shear, *J. Am. Chem. Soc.* **2010**, *132*, 13114; c) E. Sasaki, H. Kojima, H. Nishimatsu, Y. Urano, K. Kikuchi, Y. Hirata, T. Nagano, *J. Am. Chem. Soc.* **2005**, *127*, 3684.

[11] a) G. B. Richter-Addo, P. Legzdins, *Metal Nitrosyls*, Oxford University Press, New York **1992**; b) A. R. Butler, D. L. Williams, *Chem. Soc. Rev.* **1993**, *22*, 233; c) L. Jia, C. Bonaventura, J. Bonaventura, J. S. Stamler, *Nature* **1996**, *380*, 221; d) M. T. Galdwin, J. R. Lancaster Jr., B. A. Freeman, A. N. Schechter, *Nat. Med.* **2003**, *9*, 496.

[12] M. D. Pluth, E. Tomat, S. J. Lippard, *Annu. Rev. Biochem.* **2011**, *80*, 333.

[13] F.-T. Tsai, S.-J. Chiou, M.-C. Tsai, M.-L. Tsai, H.-W. Huang, M.-H. Chiang, W.-F. Liaw, *Inorg. Chem.* **2005**, *44*, 5872.

[14] a) N. J. Hinks, A. C. McKinlay, B. Xiao, P. S. Wheatley, R. E. Morris, *Microporous Mesoporous Mater.* **2010**, *129*, 330; b) A. C. McKinlay, B. Xiao, D. S. Wragg, P. S. Wheatley, I. L. Megson, R. E. Morris, *J. Am. Chem. Soc.* **2008**, *130*, 10440; c) B. Xiao, P. S. Wheatley, X. Zhao, A. J. Fletcher, S. Fox, A. G. Rossi, I. L. Megson, S. Bordiga, L. Regli, K. M. Thomas, R. E. Morris, *J. Am. Chem. Soc.* **2007**, *129*, 1203; d) P. K. Allan, B. Xiao, S. J. Teat, J. W. Knight, R. E. Morris, *J. Am. Chem. Soc.* **2010**, *132*, 3605; e) B. Xiao, P. J. Byrne, P. S. Wheatley, D. S. Wragg, X. Zhao, A. J. Fletcher, K. M. Thomas, L. Peters, J. S. O. Evans, J. E. Warren, W. Zhou, R. E. Morris, *Nat. Chem.* **2009**, *1*, 289; f) M. I. H. Mohideen, B. Xiao, P. S. Wheatley, A. C. McKinlay, Y. Li, A. M. Z. Slawin, D. W. Aldous, N. F. Cessford, T. Duren, X. Zhao, R. Gill, K. M. Thomas, J. M. Griffin, S. E. Ashbrook, R. E. Morris, *Nat. Chem.* **2011**, *3*, 304.

[15] a) P. Qin, H. J. Zhu, T. Edvinsson, G. Boschloo, A. Hagfeldt, L. C. Sun, *J. Am. Chem. Soc.* **2008**, *130*, 8570; b) Z. J. Ning, H. Tian, *Chem. Commun.* **2009**, 5483.

[16] Z. J. Tonzetich, L. E. McQuade, S. J. Lippard, *Inorg. Chem.* **2010**, *49*, 6338.

[17] S. S.-Y. Chui, S. M.-F. Lo, J. P. H. Charmant, G. Orpen, I. D. Williams, *Science* **1999**, *283*, 1148.

[18] a) L. Ma, J. M. Falkowski, C. Abney, W. Lin, *Nat. Chem.* **2010**, *2*, 838; b) Q.-R. Fang, G.-S. Zhu, Z. Jin, Y.-Y. Ji, J.-W. Ye, M. Xue, H. Yang, Y. Wang, S.-L. Qiu, *Angew. Chem. Int. Ed.* **2007**, *46*, 6638.

[19] E. Y. Lee, S. Y. Jang, M. P. Suh, *J. Am. Chem. Soc.* **2005**, *127*, 6374.

[20] L. E. McQuade, M. D. Pluth, S. J. Lippard, *Inorg. Chem.* **2010**, *49*, 8025.

[21] C. Lamberti, A. Zecchina, E. Groppob, S. Bordiga, *Chem. Soc. Rev.* **2010**, *39*, 4951.

[22] a) Y. Xiao, Y. Cui, Q. Zheng, S. Xiang, G. Qian, B. Chen, *Chem. Commun.* **2010**, *46*, 5503.

[23] a) A. C. McKinlay, R. E. Morris, P. Horcajada, G. Ferey, R. Gref, P. Couvreur, C. Serre, *Angew. Chem. Int. Ed.* **2010**, *49*, 6260; b) J. D. Rocca, D. Liu, W. Lin, *Acc. Chem. Res.* **2011**, *44*, 957.

[24] P. Wu, J. Wang, Y. Li, C. He, Z. Xie, C. Duan, *Adv. Funct. Mater.* **2011**, *21*, 2788.

[25] a) B. Zhao, X.-Y. Chen, P. Cheng, D.-Z. Liao, S.-P. Yan, Z.-H. Jiang, *J. Am. Chem. Soc.* **2004**, *126*, 15394; b) C. Serre, F. Pelle, N. Gardant, G. Ferey, *Chem. Mater.* **2004**, *16*, 1177.

[26] J. Wang, H. Wu, C. He, L. Zhao, C. Duan, *Chem. Asian J.* **2011**, *6*, 1225.

[27] a) X. Zhang, Y. Xiao, X. Qian, *Angew. Chem. Int. Ed.* **2008**, *47*, 8025; b) Z. Xu, K.-H. Baek, H. N. Kim, J. Cui, X. Qian, D. R. Spring, I. Shin, J. Yoon, *J. Am. Chem. Soc.* **2010**, *132*, 601.

[28] C. Kladis, S. K. Bhargava, K. Foger, D. B. Akolekar, *Catal. Today* **2000**, *63*, 297.

[29] S. V. Eliseevaa, J.-C. G. Bunzli, *Chem. Soc. Rev.* **2010**, *39*, 189.